IEEE Photonics Journal
An IEEE Photonics Society Publication

Open Access

Establishment and Solution for a Mathematical Model of Multiple Diffuse Reflection

Volume 12, Number 4, August 2020

Zhenmin Zhu
Xin Xu
Xiang Sun
Xinyun Wang

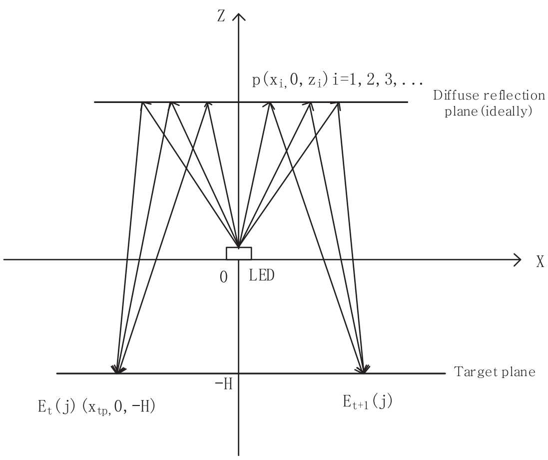

DOI: 10.1109/JPHOT.2020.3003543

Establishment and Solution for a Mathematical Model of Multiple Diffuse Reflection

Zhenmin Zhu[1], **Xin Xu**[1], **Xiang Sun**[2] and **Xinyun Wang**[1]

[1]School of Electrical and Automation Engineering, East China Jiaotong University, Nanchang 330013, China
[2]Academy for Engineering & Technology, Fudan University, Shanghai 200433, China

DOI:10.1109/JPHOT.2020.3003543

Manuscript received May 17, 2020; revised June 10, 2020; accepted June 12, 2020. Date of publication June 19, 2020; date of current version July 14, 2020. This work was supported in part by the Key Project of Industrialization of Invention Patents in Jiangxi Province under Grant 20161BBM26037, in part by the Program of Jiangxi Outstanding Youth Talent Assistance under Grant 20162BCB23047, and in part by the Science and Technology Pillar Program of Jiangxi Province under Grant 20151BBE50116.
Corresponding author: Zhenmin Zhu (e-mail: zhuzhenmin1984@163.com).

Abstract: The indirect illumination system with diffuse reflection light-emitting diode (LED) is widely applied in various fields that require high illumination uniformity. On the basis of the Lambertian characteristic of LEDs and the ideal diffuse surface, a design method that features a multiple diffuse reflectance freeform surface is proposed and its related mathematical model is established in this paper. A nonlinear algebraic equation is solved to redistribute the energy emitted by the LED to a uniformity illuminated scene. The outline of the diffuse surface is obtained by solving equations numerically. With the use of the ray tracing software TracePro, simulation results show that the effect is generally the best and the uniformity and efficiency are significantly improved compared with other methods when the proportion between the radius of the target surface and the distance between the LED light source and the target surface is 1:4.

Index Terms: Diffuse reflection, uniform illumination, freeform surface.

1. Introduction

Lighting and display are among the most important branches of technology at the beginning of the 21st century. They have changed how people think about general lighting design and application and provided important solutions for energy saving and environmental protection today and in the future [1]–[7]. Therefore, energy saving and humanization in lighting have attracted much attention. However, energy wastefulness and the human factor problem in lighting such as light pollution, glare, and non-uniform illumination are typically observed [8], [9]. To solve these problems, finding an appropriate design for luminaires is one of the most important issues in modern lighting. The problem of glare is usually solved by enlarging the effective area of the light source [10], [11]. Indirect illumination using light-emitting diodes (LEDs) and diffuse reflectors has been widely used in various fields that require uniform illumination. However, high uniformity is always achieved at the expense of light efficiency. The simultaneous multiple surface (SMS) method is an effective method of ensuing illumination efficiency [13]. This method can effectively couple two pairs of wavefronts, thus obtaining two freeform surfaces. A combiner designed by this method can typically increase the LED output by 30%–40% compared with flat-cover LEDs. Benítez [14] proposed the SMS method in 3D geometry, which provides an optical system with two freeform surfaces, thus enabling better light emission than single freeform-surface designs and improving efficiency. Hernandez [15] presented a new design of a TIR lens-mushrooms device developed with the SMS method, which also reduced loss and improved efficiency. Other methods are used to enhance the illumination efficiency. Ding [16], [17] introduced energy conservation into the design of the lens, and the desired value of the target surface is used as a condition to establish a partial differential equation. Uniformity can also be promoted by diffuse reflection.

Indirect illumination with LEDs and diffusers is widely applied in various fields that require uniform illumination. However, its high uniformity comes at the cost of sacrificing light efficiency. The diffuse reflector has the advantages of convenient material processing and high uniformity. Therefore, it is often added to non-imaging optical design to improve the uniformity of the optical system. However, the diffuse reflector is less efficient than other optical designs. Therefore, the improvement of the efficiency of the diffuse reflector is still a significant subject of research. Zhu [18], [19] introduced diffuse reflection into lighting system design. By solving a series of nonlinear algebraic equations of mathematical models, a design method of diffuse reflection freeform surface was proposed, and a mathematical model of diffuse reflection hemisphere based on circular LED array was established. Compared with traditional direct illumination, this method greatly improved the uniformity and efficiency of diffuse reflection hemisphere surfaces. However, the theory of diffuse reflection still needs to be further improved. Therefore, Zhu [20], [21] adopted energy-saving measures, which greatly compensated for the inefficiency of the design. With the use of the bidirectional reflectance distribution function (BRDF) of the inner surface of a diffuse freeform surface, a mathematical simulation algorithm was established to represent the radiation of the irradiated plane. The expected values on the target plane were calculated according to the conservation law, and a set of nonlinear algebraic equations was established. Compared with the traditional design methods (direct lighting and diffuse illumination with hemispherical inner surface), better uniformity and higher efficiency were obtained. Then, a method of designing diffuse reflective asymmetric surfaces was proposed [22], which could be used to obtain different asymmetric surfaces for different LED arrays. Compared with the traditional methods, this method improved not only the efficiency but also the uniformity. Moreover, in the far-field situation, the efficiency of the proposed surface for hexagonal LED array can reach 70.86%, while the rotational symmetry is 64.73%, and the direct irradiation is only 47.59%.

In this paper, a series of mathematical models for the reflection of light on a diffuse freeform surface is presented. These models mainly consider diffuse reflection plane, first diffuse reflection freeform, second diffuse reflection freeform and third diffuse reflection freeform surfaces. In Sections 2.1, 2.2, and 2.3, the related mathematical models are mainly introduced. A mathematical model of multiple diffuse reflectance is established. The designed diffuse reflectance freeform surface redistributes the energy emitted by the LED to obtain a uniform illumination area on the target plane. On the basis of the law of conservation of energy, the expected value uniformity on the target plane is calculated, and then a mathematical simulation algorithm is established to represent the radiation of the irradiated plane by using the bidirectional scattering distribution function of the diffuse freeform surface. A set of nonlinear algebraic equations is established according to the expected values on the target plane calculated by the conservation law. The relevant diffuse reflector plane, the primary diffuse reflector freeform surface, the secondary diffuse reflector freeform surface, and the cubic diffuse reflector freeform surface are established by using this method. Experimental results show that the uniformity and efficiency are nearly maximum at about 86% and higher uniformity and efficiency are obtained compared with traditional methods when the third diffuse reflection occurs.

2. Design Method of the Diffuse Reflection Freeform Surface

In order to construct the mathematical simulation algorithm of the whole system, it is necessary to establish a single LED illumination model. The radius of ordinary LED chip is generally between

1 mm and 3 mm, and the whole system size is larger than the radius of LED chip, so a single LED chip can be regarded as a point light source in the whole diffuse illumination system. Ideally, the radiant intensity of LED point light source can be expressed as shown in Eq. (1):

$$E(r,\theta) = E_0(r)\cos^m\theta \tag{1}$$

Where θ is the angle between the light and the optical axis; r is the distance between LED and illuminated area, $E_0(r)$ is the irradiance distribution at a distance d and $\theta = 0^\circ$, the value of d is d is the distance from the LED to the illumination plane, and the value of m is related to the relative position of the region where the center of curvature of the spherical package of the LED emits light. If the position of the chip coincides with the center of curvature, $m = 1$, the LED can be approximated as a Lambert. In practice, the value of m of a typical LED is greater than 1, and is related to the angle θ, which can be determined by the half-intensity light angle $\theta_{1/2}$. The half-intensity light angle $\theta_{1/2}$ can be obtained from the LED manufacturer. It can be defined as the angle between the light and the optical axis when the radiation intensity is half of the radiation intensity in the direction of $\theta = 0^\circ$. When $\theta = \theta_{1/2}$, $E(r,\theta) = E_0(r)/2$, substituting into the Eq. (1), the m value can be expressed by:

$$m = \frac{-\ln 2}{\ln(\cos\theta_{1/2})} \tag{2}$$

When the LED is illuminated onto a plane perpendicular to its optical axis, the irradiance distribution E which gives by Eq. (1) can be further adapted as:

$$E\,(r,\theta) = \frac{I_0 cos^m\theta}{d^2} \tag{3}$$

Where I_0 is the radiant intensity (W/sr) of the LED along the normal direction, d is the distance from the LED to the illumination plane. When the irradiance distribution of single LED given by Eq. (1) illuminates a point on the plane, the equation is transformed into a Cartesian coordinate system (x, y, z), and Eq. (3) can be transformed into:

$$E\,(x,y,z) = \frac{z^m I_0}{\left[(x-x_i)^2 + (y-y_i)^2 + z^2\right]^{(m+2)/2}} \tag{4}$$

Where (x_i, y_i) is the position coordinate of the LED, Eq. (4) is the irradiance distribution model of single LED.

2.1 Diffuse Reflection Plane (Ideally)

In this paper, it is considered that the diffuse reflection freeform surface has rotational symmetry. Therefore, we consider the 2-D model and take the ***X-Z*** plane as an example. Fig. 1 shows the points on the diffuse reflection freeform plane ***P*** and target plane ***T*** can be further represented as $p(x_i, 0, z_i)$ and $E_t(j)(x_{tp}, 0, -H)$ on the 2-D plane of ***X-Z***. According to the knowledge of space vector, we can get:

$$\begin{cases} \overrightarrow{\boldsymbol{OUT}} = \left(x_{tp} - x_i, -H - z_i\right) \\ \vec{\boldsymbol{N}} = (-1, 0) \\ cos\partial = \frac{\overrightarrow{\boldsymbol{OUT}}\cdot\vec{\boldsymbol{N}}}{\left|\overrightarrow{\boldsymbol{OUT}}\right|\cdot|\vec{\boldsymbol{N}}|} \end{cases} \tag{5}$$

Where $\overrightarrow{\boldsymbol{OUT}}$ is the vector that represents the emergent ray from point p and t after reflection by P, $\vec{\boldsymbol{N}}$ is the normal vector of P at point p, ∂ is the angle between $\overrightarrow{\boldsymbol{OUT}}$ and $\vec{\boldsymbol{N}}$.

Lambert surface can be defined as a surface with constant illumination in any direction, and its hemispheric reflectance is 1. Since the hemispherical surface is a highly diffuse reflective surface, it can be approximately seen as a Lambertian surface. For Lambert's surface there are:

$$I_\partial = I_0 cos\partial \tag{6}$$

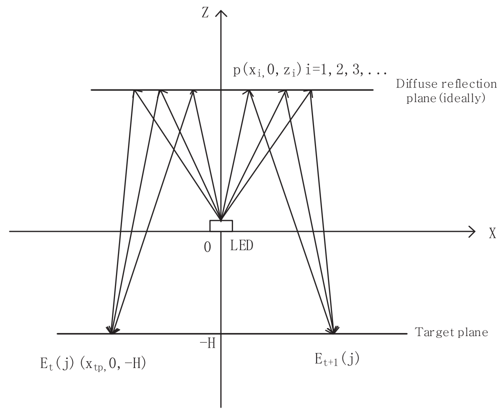

Fig. 1. Schematic diagram of the diffuse reflection plane (ideally).

Where I_∂ is the emergent light intensity in a certain emitting-angle ∂. Accordingly, the irradiance distribution on the target plane can be given by the following formula:

$$E' = \int \frac{E \cdot BRDF \cdot cos\partial \cdot dS}{d'^2} \tag{7}$$

Where E is the received irradiance of the freeform surface given by Eq. (4), d' is the distance between the freeform surface and the direction plane, dS represents the area element on the freeform surface. The $BRDF$ is bidirectional reflectance distribution function, which used to represent the freeform surface reflectance properties. It can be given by:

$$BRDF = \frac{\omega}{\pi} \tag{8}$$

Where ω is the diffuse reflectance ratio of the freeform surface. To simplify the calculation, the reflected irradiance distribution of the target plane given by Eq. (7) in complex integral from is replaced by a simple irradiance superposition from all these secondary sources:

$$E' = \sum_{i=1}^{N} \frac{E\left(x_i, 0, z_i\right) \Delta BRDF \Delta cos\partial_i}{d'^2} \tag{9}$$

Where N is the number of discrete points in the intersection. Then substituting Eq. (5) and Eq. (8) into Eq. (9), the illumination of a single discrete point on the target plane is obtained as shown in Eq. (10):

$$E\left(x_{tp}, 0, -H\right) = \sum_{i=1}^{N} \frac{E\left(x_i, 0, z_i\right) \cdot \omega \cdot \left(x_i - x_{tp}\right)}{\pi \cdot \left[\left(x_{tp} - x_i\right)^2 + \left(H + z_i\right)^2\right]^{3/2}} \tag{10}$$

2.2 First Diffuse Reflection Freeform Surface

Fig. 2 shows the points on the diffuse reflection freeform surface $\boldsymbol{P}$ and target plane $\boldsymbol{T}$ can be further represented as $p(x_i, 0, z_i)$ and $T(x_{tp}, 0, -H)$ on the 2-D plane of $\boldsymbol{X}$-$\boldsymbol{Z}$. According to the knowledge of space vector, we can get:

$$\begin{cases} \overrightarrow{\boldsymbol{OUT}} = \left(x_{tp} - x_i, -H - z_i\right) \\ \vec{\boldsymbol{N}} = (-dz, dx) \\ cos\partial = \frac{\overrightarrow{\boldsymbol{OUT}} \cdot \vec{\boldsymbol{N}}}{\left|\overrightarrow{\boldsymbol{OUT}}\right| \cdot \left|\vec{\boldsymbol{N}}\right|} \end{cases} \tag{11}$$

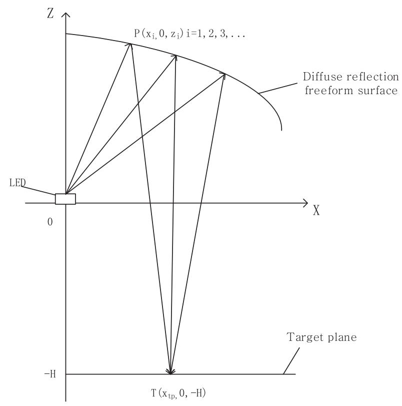

Fig. 2. Schematic diagram of the diffuse reflection freeform surface for the first diffuse reflection occurs.

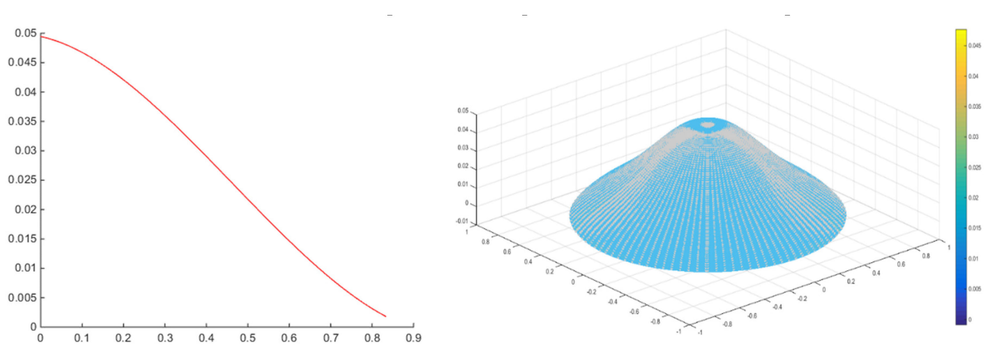

Fig. 3. The diffuse reflection freeform surface 2D contours and 3D diffuse reflection freeform surface for for the first diffuse reflection occurs.

Then substituting Eq. (8) and Eq. (11) into Eq. (9), the irradiance simulated algorithm of the point $T(x_{tp}, 0, -H)$ on the target plane can be reduced as shown in Eq. (12):

$$E'\left(x_{tp}, 0, -H\right) = \sum_{i=1}^{N} \frac{E\left(x_i, 0, z_i\right) \cdot \omega \cdot \left[\left(x_{tp} - x_i\right) \cdot \left(Z_{i+1} - Z_i\right) + \left(H + Z_i\right) \cdot \left(x_{i+1} - x_i\right)\right]}{\pi \cdot \left[\left(x_{tp} - x_i\right)^2 + \left(H + z_i\right)^2\right]^{3/2} \left[\left(z_{i+1} - z_i\right)^2 + \left(x_{i+1} - x_i\right)^2\right]^{1/2}} \tag{12}$$

With the continuous improvement of high-power LED emission intensity, the lighting system using single LED as point light source has been widely used. On the basis of the theory of differential geometry, a series of partial nonlinear equations are established, and according to the energy mapping relations between source and the target plane are established. The points of the surface are obtained by solving the differential equations with Matlab (Version 2014). Fig. 3 shows the 2-D contour of a freeform surface when the first diffuse reflection occurs. The desired freeform surface is constructed by using the obtained surface data in the 3-D modeling software Solidworks (Version 2015). Fig. 4 shows the surface shape of a freeform surface when the first diffuse reflection occurs. The obtained freeform surface is imported into the optical simulation software Tracepro (Version 7.4.3) for simulation.

2.3 Second Diffuse Reflection Surface

Fig. 4 shows the points on the diffuse reflection freeform surface ***P*** and target plane ***T*** can be further represented as $p(x'_i, 0, z'_i)$ and $T(x'_{tp}, 0, -H)$ on the 2-D plane of ***X-Z***. In this paper, assuming that there are N radiation points on the diffuse reflector freeform surface, the radiation illumination value

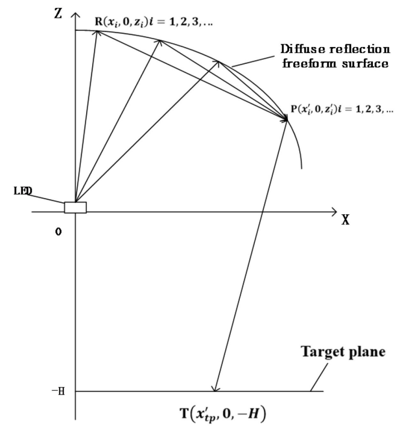

Fig. 4. Schematic diagram of the diffuse reflection freeform surface for second diffuse reflection occurs.

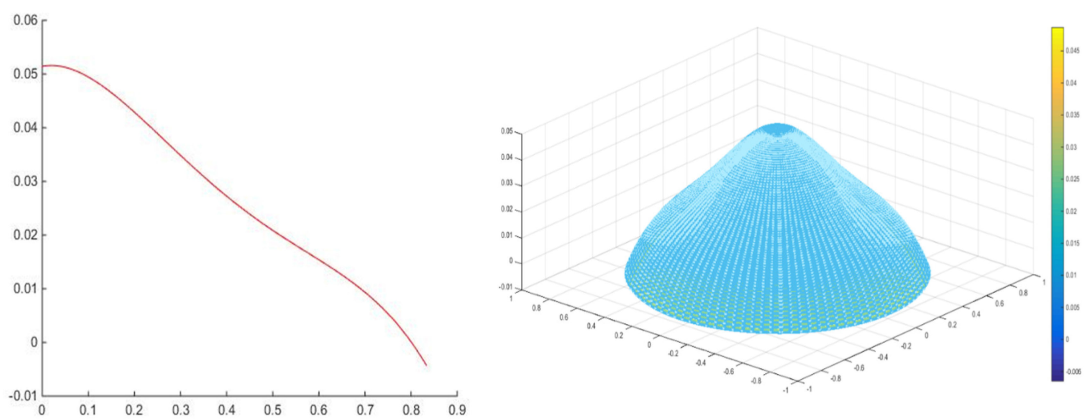

Fig. 5. The diffuse reflection freeform surface 2D contours and 3D diffuse reflection freeform surface for the second diffuse reflection occurs.

of each point is E_i, and each radiation point radiates to two non-adjacent points. We can get:

$$\begin{cases} 1 : E_1 = \sum_{i=3}^{N} E_i \\ 2 : E_2 = \sum_{i=4}^{N} E_i \\ \vdots \\ i-1 : E_{i-1} = \sum_{i=1}^{N-3} E_i \\ i : E_i = \sum_{i=1}^{N-2} E_i \end{cases} \tag{13}$$

Combining the Eq. (8), Eq. (9), Eq. (12) and Eq. (13), the irradiance simulated algorithm of the point $T(x'_{tp}, 0, -H)$ on the target plane can be reduced as shown in Eq. (14):

$$E_2\left(x'_{tp}, 0, -H\right) = \sum_{i=1}^{N} \frac{E'\left(x_{tp}, 0, -H\right) \cdot \omega \cdot \left[\left(x'_{tp} - x'_i\right) \cdot \left(z'_{i+1} - z'_i\right) + \left(H + z'_i\right) \cdot \left(z'_{i+1} - x'_i\right)\right]}{\pi \cdot \left[\left(x'_{tp} - x'_i\right)^2 + \left(H + z'_i\right)^2\right]^{3/2} \left[\left(z'_{i+1} - z'_i\right)^2 + \left(z'_{i+1} - x'_i\right)^2\right]^{1/2}} \tag{14}$$

The points of the surface are obtained by solving the differential equations with Matlab (Version 2014). Fig. 5 shows the 2-D contour of a freeform surface when the second diffuse reflection occurs. The desired freeform surface is constructed by using the obtained surface data in the 3-D modeling

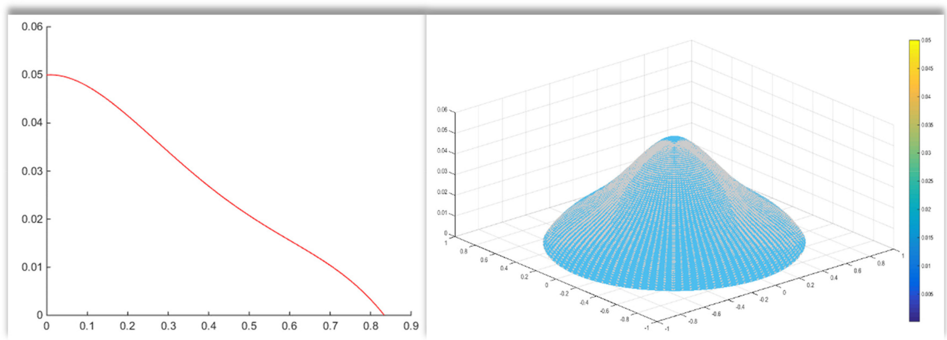

(a)

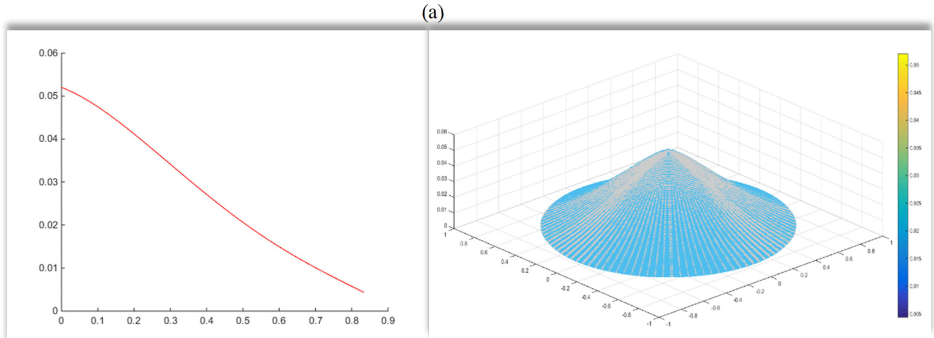

(b)

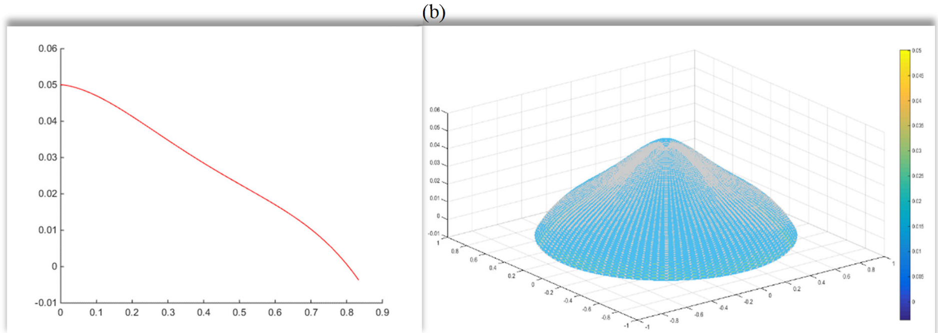

(c)

Fig. 6. Seven different diffuse freeform surface models in the case of third diffuse reflection.

software Solidworks (Version 2015). Fig. 5 shows the surface shape of a freeform surface when the second diffuse reflection occurs. The obtained freeform surface is imported into the optical simulation software Tracepro (Version 7.4.3) for simulation.

2.4 Third Diffuse Reflection Surface

The same can be obtained, according to the second diffuse reflection formula in the part III, we can get:

$$E_3\left(x''_{tp}, 0, -H\right) = \sum_{i=1}^{N} \frac{E_2\left(x'_{tp}, 0, -H\right) \cdot \omega \cdot \left[\left(x''_{tp} - x''_i\right) \cdot \left(z''_{i+1} - z''_i\right) + \left(H + z''_i\right) \cdot \left(x''_{i+1} - x''_i\right)\right]}{\pi \cdot \left[\left(x''_{tp} - x''_i\right)^2 + \left(H + z''_i\right)^2\right]^{3/2} \left[\left(z''_{i+1} - z''_i\right)^2 + \left(x''_{i+1} - x''_i\right)^2\right]^{1/2}} \tag{15}$$

Diffuse reflection is the reflection of light projected on a rough surface in all directions. When a parallel beam of incident light strikes a rough surface, the surface will reflect the light in all

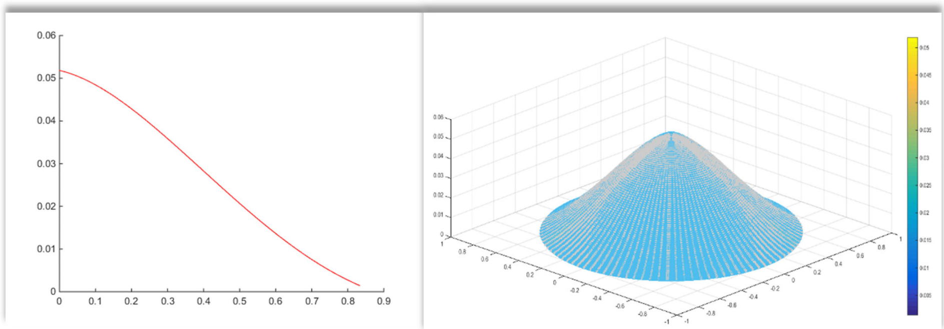

(d)

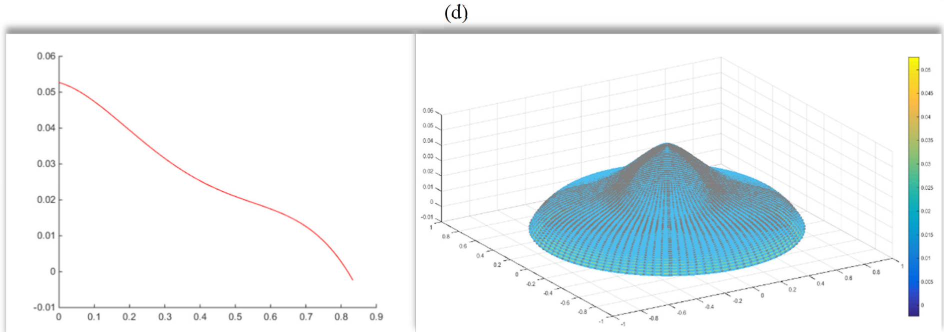

(e)

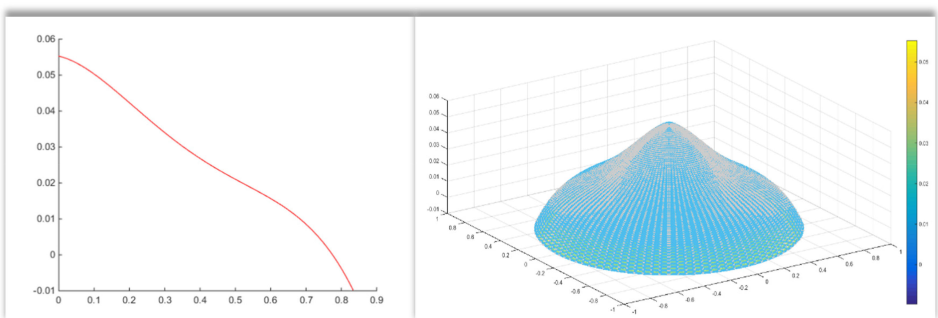

(f)

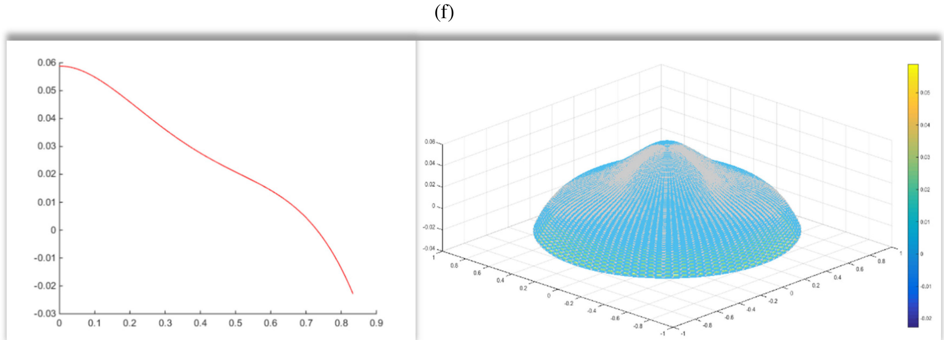

(g)

Fig. 6. Continued.

directions. Therefore, although the incident rays are parallel to each other, the reflected light is reflected irregularly in different directions due to the different normal directions of each point. This reflection is called diffuse reflection and the reflected light is called diffuse light. Many objects, such as plants, walls, and clothes seem to have a continuous rough surface, but a closer look at them with a magnifying glass shows that their surface is uneven. Thus, the parallel sunlight is reflected by these surfaces, diffusely shining in different directions.

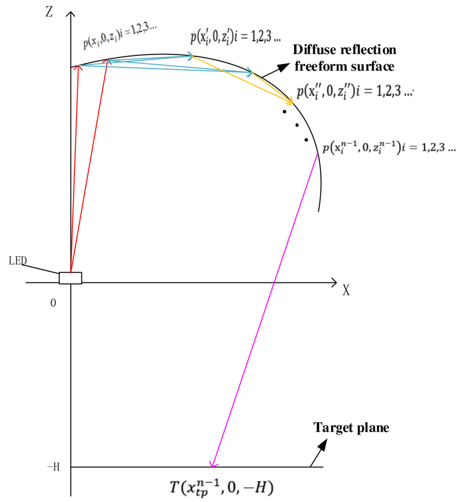

Fig. 7. Schematic diagram of the diffuse reflection freeform surface for nth diffuse reflection occurs.

To prove the validity of the paper more effectively, this paper establishes several different mathematical models under the condition of distance Z = 400 mm and R = 100 mm, Z is the distance between the LED light source and the target illumination surface, and R is the radius of the target illumination surface, as shown in the following Fig. 6.

2.5 NTH Diffuse Reflection Surface

As shown in Fig. 7, the points on the diffuse reflection freeform surface ***P*** and target plane ***T*** can be further represented as $p(x_i^{n-1}, 0, z_i^{n-1})$ and $T(x_{tp}^{n-1}, 0, -H)$ on the 2-D plane of ***X-Z***. In this paper, assuming that there are N radiation points on the diffuse reflector freeform surface, the radiation illumination value of each point is E_i, and each radiation point radiates to two non-adjacent points.

Therefore, according to the above diffuse freeform surface, we can further obtain that when the nth diffuse occurs, the illuminance distribution of the diffuse freeform surface on the target illumination surface is:

$$E_n\left(x_{tp}^{n-1}, 0, -H\right) = \sum_{i=1}^{N} \frac{E_{n-1}\left(x_{tp}^{n-2}, 0, -H\right) \cdot \omega \cdot \left[\left(x_{tp}^{n-1} - x_i^{n-1}\right) \cdot \left(z_{i+1}^{n-1} - z_i^{n-1}\right) + \left(H + z_i^{n-1}\right) \cdot \left(x_{i+1}^{n-1} - x_i^{n-1}\right)\right]}{\pi \cdot \left[\left(x_{tp}^{n-1} - x_i^{n-1}\right)^2 + \left(H + z_i^{n-1}\right)^2\right]^{3/2} \left[\left(z_{i+1}^{n-1} - z_i^{n-1}\right)^2 + \left(x_{i+1}^{n-1} - x_i^{n-1}\right)^2\right]^{1/2}} \tag{16}$$

3. Simulation Results and Discussion

For the above seven diffuse freeform surface models, in order to obtain the best model, it is necessary to verify the accuracy of all models under various parameters. As shown in the following Table 1 and Table 2.

It can be seen from the above table that the third diffuse freeform surface of type c selected in this design can get the best results in most parameters of Z and R. In the same way, the efficiency of different diffuse freeform surfaces under various parameters has little difference. To carry out further simulation experiments, type c freeform surface is selected as the optimal freeform surface in the third diffuse freeform surface model.

TABLE 1
Uniformity of Seven Kinds of Diffuse Freeform Surfaces Under Various Parameters in Fig. 8

	Uniformity						
	a	b	c	d	e	f	g
Z=150,R=40	82.34%	83.20%	**84.51%**	84.41%	83.63%	83.04%	81.08%
Z=200,R=40	81.65%	80.84%	**82.98%**	82.19%	81.26%	81.49%	78.66%
Z=200,R=50	83.21%	83.08%	**84.62%**	84.14%	82.93%	83.08%	80.64%
Z=300,R=100	82.90%	83.06%	**83.07%**	82.43%	82.57%	82.69%	81.59%
Z=400,R=100	82.05%	83.42%	**85.29%**	83.86%	82.92%	82.65%	80.35%
Z=400 R=150	81.27%	81.71%	**81.84%**	81.00%	81.28%	81.50%	80.29%
Z=600,R=150	82.44%	83.49%	**85.24%**	83.70%	83.12%	82.35%	80.58%
Z=800,R=150	81.50%	79.22%	81.49%	**81.77%**	80.48%	80.99%	78.69%
Z=600,R=200	82.95%	82.92%	**83.10%**	82.45%	82.68%	82.61%	81.57%
Z=800,R=200	82.23%	83.51%	**85.31%**	83.58%	83.22%	82.38%	80.55%
Z=1200,R=400	82.71%	**83.22%**	83.16%	82.35%	82.67%	82.84%	81.23%
Z=1600,R=400	82.32%	83.25%	**85.34%**	83.61%	83.21%	82.49%	80.44%

When we obtained the freeform surface, TracePro (Version 7.4.3) is used to simulate and verify the results of the diffuse transmissive freeform surface illumination performance. Here, a single LED at the origin can be treated as the source for the simulation and the LED has an analogous Lambertian radiation distribution, with the die size of 1 mm $\times$ 1 mm and the power of the single LED is 1Watt. Compared with the size of the free-form surface, the LED can be regarded as a point light source. In this simulation experiment, the distance between the LED light source and the target illumination surface is between 150 mm and 1600 mm. Table 3 shows the uniformity and efficiency of Fig. 7 under seven different diffuse freeform surface models at distance Z $=$ 400 mm and R $=$ 100 mm. From the table, it can be seen that the efficiency of the seven models is not much different, all of which are about 5.83%. For uniformity, the uniformity of model *c* is the highest, reaching 85.29%.

Fig. 8 shows the simulated results of ray-tracing simulation with Z $=$ 600 mm. Meanwhile, the simulation results of different distances and radius further show the importance of the method in Table 2. It shows that the efficiency and uniformity of the target plane get better under different conditions. By adjusting the illumination distance and the size of the target plane, we compare four kinds of diffuse reflective surface, which are diffuse reflection plane, first diffuse reflection, second diffuse reflection, third diffuse reflection, to verify the validity of the design method of the surface. From Fig. 8, we can see that the illumination uniformity is 84.49% under the condition of Z $=$ 600 mm, which is suitable for various fields requiring uniform illumination.

To prove the correctness and accuracy of our research, we selected several sets of data for comparison. On the basis of the results, we can conclude that this paper has a certain significance. Table 4 shows the lighting efficiency and uniformity of four lighting methods (diffuse reflection plane,

TABLE 2
Efficiency of Seven Kinds of Diffuse Freeform Surfaces Under Various Parameters in Fig. 8

	Efficiency						
	a	b	c	d	e	f	g
Z=150,R=40	6.57%	6.57%	6.57%	6.57%	6.57%	6.58%	6.60%
Z=200,R=40	3.81%	3.81%	3.81%	3.81%	3.81%	3.81%	3.82%
Z=200,R=50	5.83%	5.83%	5.83%	5.83%	5.83%	5.83%	5.83%
Z=300,R=100	9.91%	9.90%	9.91%	9.90%	9.91%	9.93%	9.96%
Z=400,R=100	5.83%	5.82%	5.83%	5.83%	5.83%	5.83%	5.85%
Z=400,R=150	12.20%	12.20%	12.20%	12.20%	12.21%	12.23%	12.26%
Z=600,R=150	5.83%	5.83%	5.83%	5.83%	5.83%	5.83%	5.85%
Z=800,R=150	3.37%	3.36%	3.37%	3.36%	3.37%	3.37%	3.38%
Z=600,R=200	9.91%	9.91%	9.91%	9.91%	9.92%	9.93%	9.96%
Z=800,R=200	5.83%	5.82%	5.83%	5.82%	5.83%	5.83%	5.85%
Z=1200,R=400	9.91%	9.91%	9.91%	9.91%	9.92%	9.93%	9.96%
Z=1600,R=400	5.83%	5.82%	5.83%	5.83%	5.83%	5.83%	5.85%

TABLE 3
Illumination Uniformity and Efficiency of Seven Different Models of Diffuse Freeform Surface in Fig. 5

Diffuse Reflection Freeform Surface Model	Uniformity	Efficiency
a	82.05%	5.83%
b	83.42%	5.82%
c	85.29%	5.83%
d	83.86%	5.83%
e	82.92%	5.83%
f	82.65%	5.83%
g	80.35%	5.85%

first diffuse reflection, second diffuse reflection, and third diffuse reflection). With the increase in the source–target distance, the uniformity of traditional systems becomes unstable. In this paper, the illumination uniformity of the diffuse reflection freeform surface is higher than that of the other lighting systems. At the same distance and different radius of the target plane, the illumination uniformity is higher than that of other lighting systems. When the source–target distance is $Z = 200$ mm and the radius of the target plane is 50 mm, the uniformity of illumination reaches the maximum. Simulation results show that when the radius of the target surface and the distance

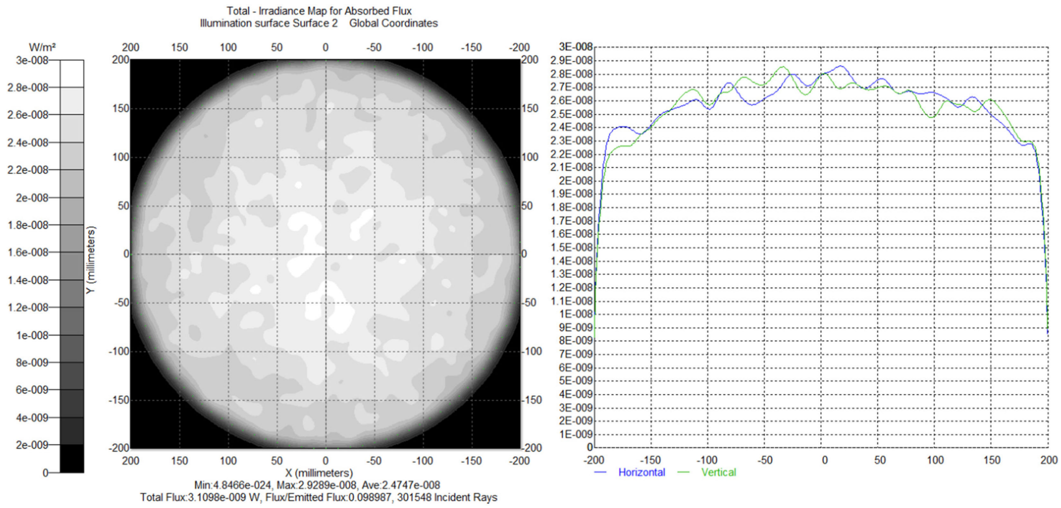

(a) (b)

Fig. 8. Simulation results of the irradiation uniformity over the target plane at the distance Z = 600 mm. (a) the irradiation distribution of the illumination scene which is a circular area with the radius R = 600 mm. (b) the uniformity across the center of the target plane along x axis and y axis.

TABLE 4
Illumination Uniformity and Efficiency of Four Lighting Methods

	Uniformity				Efficiency			
	diffuse reflection plane	first diffuse reflection freeform	second diffuse reflection freeform	third diffuse reflection freeform	diffuse reflection plane	first diffuse reflection freeform	second diffuse reflection freeform	third diffuse reflection freeform
Z=150,R=40	81.43%	82.84%	84.17%	**84.41%**	5.29%	6.36%	6.48%	**6.57%**
Z=200,R=40	77.07%	80.08%	82.44%	**82.68%**	2.30%	3.75%	3.81%	**3.81%**
Z=200,R=50	79.89%	82.18%	85.25%	**85.36%**	5.10%	5.63%	5.83%	**5.83%**
Z=300,R=100	79.50%	80.93%	83.48%	**84.77%**	5.67%	9.34%	9.76%	**9.77%**
Z=400,R=100	79.77%	80.67%	84.35%	**85.29%**	3.15%	5.48%	5.83%	**5.83%**
Z=400,R=150	79.93%	80.24%	81.97%	**82.03%**	9.34%	11.51%	12.2%	**12.2%**
Z=600,R=150	79.58%	82.31%	84.80%	**85.24%**	4.02%	5.63%	5.82%	**5.83%**
Z=800,R=150	76.86%	79.65%	81.45%	**81.43%**	2.30%	3.25%	3.36%	**3.37%**
Z=600,R=200	79.97%	80.60%	83.39%	**84.49%**	8.53%	9.90%	9.90%	**9.90%**
Z=800,R=200	81.84%	82.44%	84.16%	**85.31%**	4.16%	5.51%	5.63%	**5.83%**
Z=1200,R=400	80.01%	81.40%	83.34%	**84.82%**	7.84%	9.36%	9.20%	**9.78%**
Z=1600,R=400	81.20%	82.98%	85.33%	**85.34%**	4.30%	5.48%	5.84%	**5.84%**

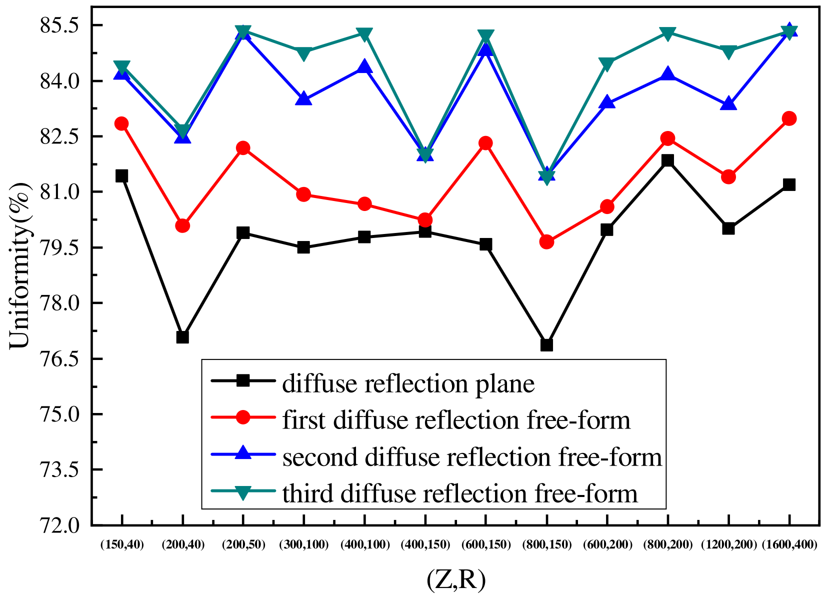

Fig. 9. Simulation results with different illumination schemes and at different source-target distances irradiation uniformity over the target plane.

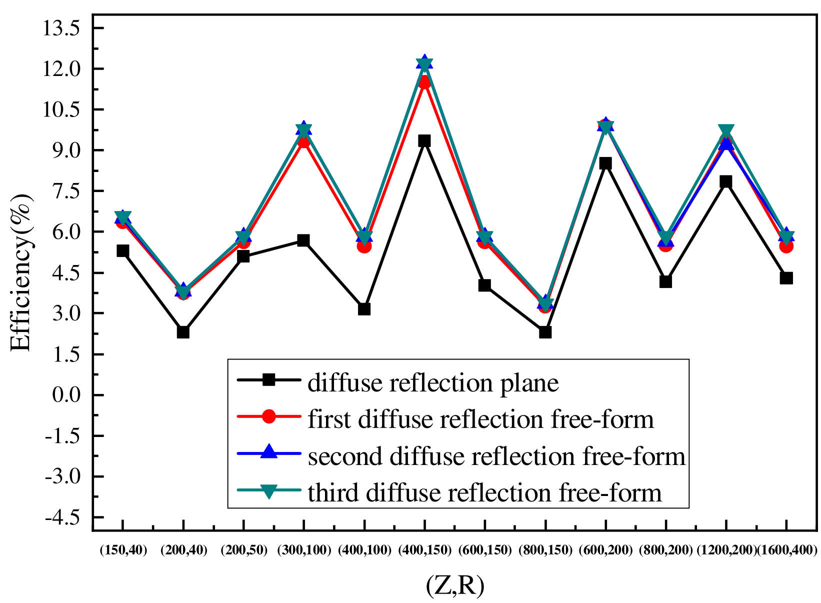

Fig. 10. Simulation results with different illumination schemes and at different source-target distances irradiation efficiency over the target plane.

between the source and the target surface is 1:4, the effect is generally the best. After three diffuse reflections, the uniformity can reach about 85.36%.

Fig. 9 shows the simulation results with different illumination schemes and at different source-target distances irradiation uniformity over the target plane.

Fig. 10 shows the simulation results with different illumination schemes and at different source-target distances irradiation efficiency over the target plane. We can find the efficiency of the second

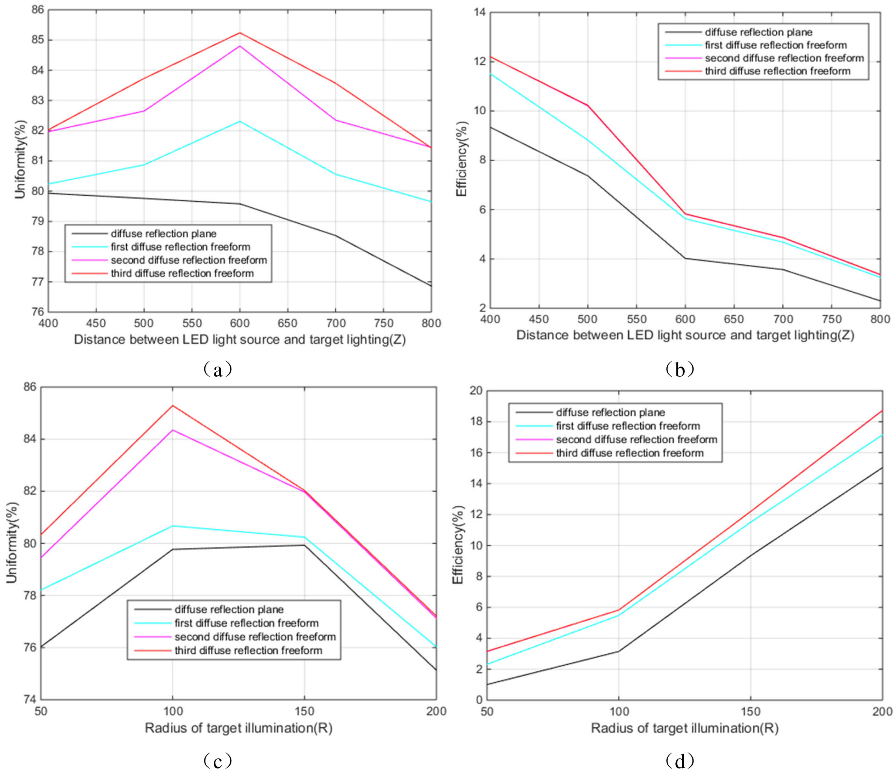

Fig. 11. (a) Uniformity of different illumination distances when the target plane radius is 150 mm. (b) Lighting efficiency at different lighting distances with a target surface radius of 150 mm. (c) Illumination uniformity of different target plane radii with illumination distance of 400 mm. (d) Illumination efficiency of different target plane radii with illumination distance of 400 mm.

diffuse reflection and the third diffuse reflection are very close to each other. When the source–target distance is Z = 400 mm, and the radius of the target plane is 150 mm, the efficiency of illumination reaches the maximum.

Fig. 11 shows the illumination uniformity and efficiency of different diffuse freeform surfaces under different conditions. Evidently, the lighting condition of each lighting system changed with the increasing distance between the light source and the target plane. Figs. 11(a) and 11(b) show the variation trend of uniformity and efficiency of different lighting systems when the radius of the target lighting surface is unchanged and the illumination distance is changed. The illumination efficiency of four different diffuse freeform surfaces decreases with the increasing distance between the light source and the target illumination surface. However, the illumination efficiency of the three diffuse freeform surfaces is higher than that of the other three forms. The radius of the target illumination surface changes when the distance between the control light source and the target illumination surface is constant. Figs. 11(c) and 11(d) clearly show that the irradiance uniformity of the system reaches the maximum value when the distance Z between the light source and the target illumination surface is maintained at 400 mm and the radius of the target plane reaches 100 mm. The irradiance uniformity of the system reaches the maximum value when the radius r of the target illumination surface is maintained at 150 mm, and the distance between the light source and the target illumination surface reaches 600 mm. Similarly, when the radius of the target illumination surface is maintained at 150 mm, the illumination efficiency of the system will gradually decrease with the increasing distance between the light source and the target illumination surface. When the distance between the light source and the target illumination surface is maintained at 400 mm, the illumination efficiency of the system will gradually increase with the increasing radius of the target illumination surface.

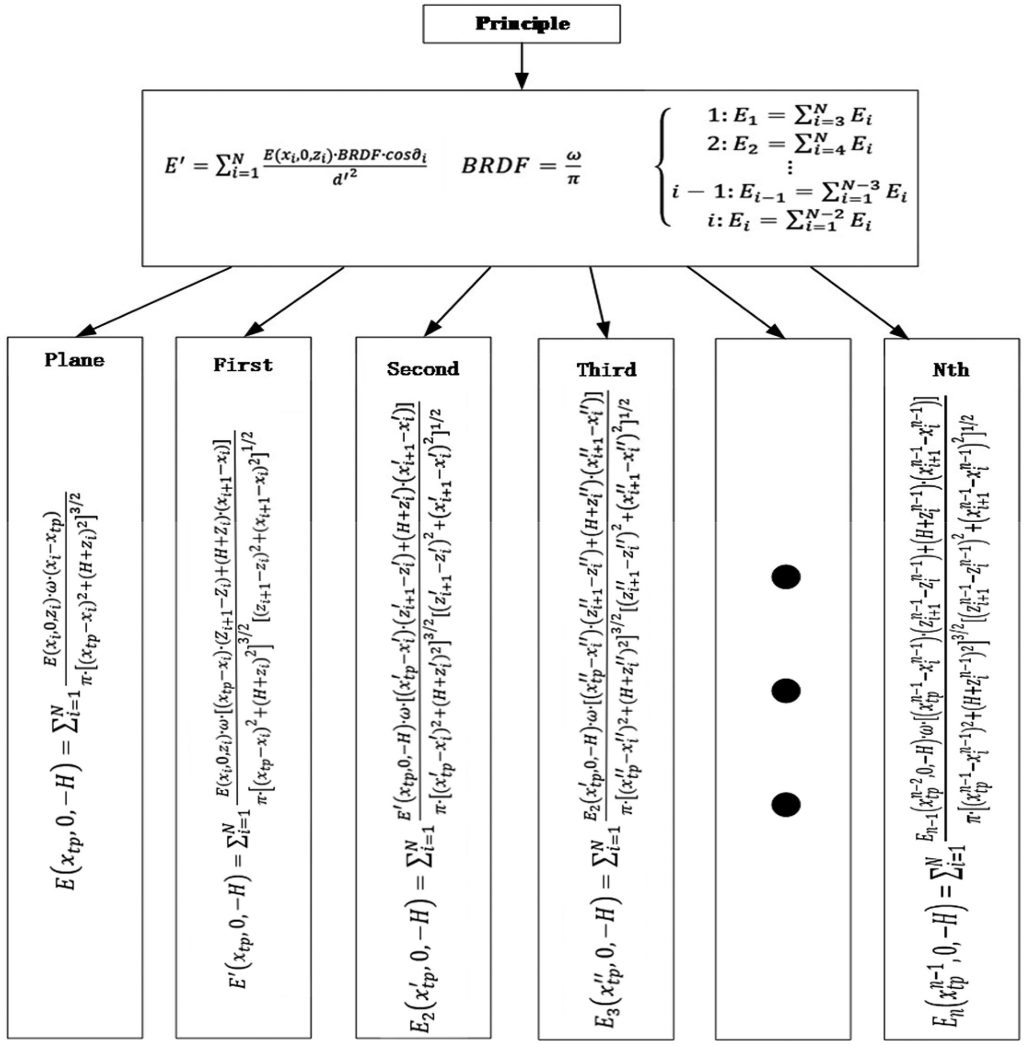

Fig. 12. Association and implementation of various diffuse freeform surfaces.

From Fig. 12, for the diffuse plane (ideal case) and the diffuse freeform surface obtained when one diffuse occurs, the light source is emitted from the LED; after light passes through the diffuse freeform surface, only one reflection occurs and then reaches the target lighting surface. At this time, the diffuse plane and the diffuse freeform surface can be obtained according to the corresponding expression. Diffuse reflection is the reflection of light on a rough surface in all directions. When a beam of parallel incident light strikes a rough surface, the surface will reflect the light in all directions. Although the incoming rays are parallel to each other, the normal directions of each point are not the same, resulting in the light being reflected irregularly in different directions. Therefore, on the basis of this theory, this paper considers the existence of multiple diffuse reflections. When the second diffuse occurs, as shown in Fig. 4, the light emitted by the light source from the LED reaches the R point on the diffuse freeform surface. At this time, the R point is equivalent to a Lambert body light source that continues to reflect to the diffuse freeform surface to the P point. By the same principle, a series of R and P points of the diffuse freeform surface begins to occur. The following principle is obeyed: Each radiation point radiates to two non-adjacent points. After a series of irradiance superposition, the freeform surface is obtained when the secondary diffuse reflection occurs when light arrives at the T-point of the illuminating surface of the target surface, and the

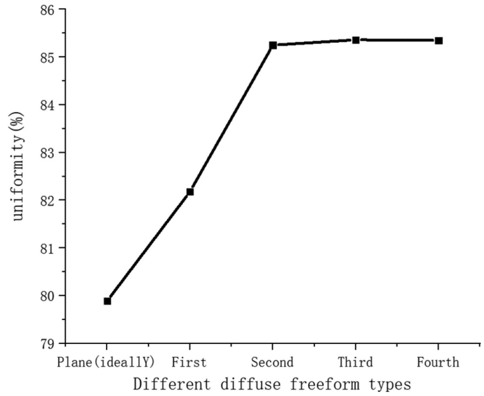

Fig. 13. Comparison of simulation results between diffuse reflector plane and diffuse reflector freeform surface.

corresponding multiple diffuse freeform surface is obtained by applying its rules to the cases of secondary, tertiary, and multiple diffuse reflection. Finally, the simulation results are analyzed and compared.

In accordance with the above methods, we choose a suitable mathematical model of the fourth diffuse reflectance freeform surface and conduct an optical simulation experiment on the model. The experimental results are compared with those of the previous three diffuse reflectance mathematical models. The results are shown in Fig. 13.

From Fig. 13, we can see that the best effect is achieved when the third diffuse reflection freeform surface occurs, that is, when the fourth diffuse reflection occurs, the energy is consumed in the process of reflection.

4. Conclusion

In this paper, a model of a multiple diffuse reflectance freeform surface is established based on the design of diffuse reflectance freeform surface. The simulation results show that when the distance between the target surface and the light source is 4:1 in proportion to the radius of the target surface, the uniformity is generally the highest, and when the third diffuse reflection occurs, the maximum uniformity and efficiency are achieved. Compared with the other three methods, the proposed model has better fault tolerance and stability in terms of illumination uniformity and efficiency. The simulation results show that the uniformity of the illuminated circular area on the target illumination surface is close to 86%, and the light output efficiency is better than that of the traditional light source. The diffuse reflector freeform lens designed in this work has high illumination uniformity and light output efficiency, thereby providing economic benefits to LED lighting projects. For diffuse indirect illumination, the significant improvement of efficiency and uniformity can increase the utilization of illumination systems to a certain extent.

Disclosures: The authors declare no conflicts of interest.

References

[1] J. Jiang *et al.*, "Optical design of a freeform TIR lens for LED streetlight," *Optik - Int. J. Light Electron Opt.*, vol. 121, no. 19, pp. 1761–1765, 2010.
[2] C. W. Chiang, Y. K. Hsu, and J. W. Pan, "Design and demonstration of high efficiency anti-glare LED luminaires for indoor lighting opt," *Opt. Express*, vol. 23, pp. 12–23, 2015.
[3] C. H. Tsuei, J. W. Pen and W. S. Sun, "Simulating the illuminance and the efficiency of the led and fluorescent lights used in indoor lighting design," *Opt. Express*, vol. 16, pp. 18692–701, 2008.
[4] H. C. Chen, J. Y. Lin, and H. Y. Chiu, "Rectangular illumination using a secondary optics with cylindrical lens for LED street light," *Opt. Express*, vol. 21, no. 3, pp. 3201–3212, 2013.

[5] Z. Feng, Y. Luo, and Y. Han, “Design of LED freeform optical system for road lighting with high luminance/illuminance ratio,” *Opt. Express*, vol. 18, no. 21, pp. 22020–22031, 2010.
[6] H. C. Chen, J. Y. Lin, and H. Y. Chiu, “Rectangular illumination using a secondary optics with cylindrical lens for LED street light,” *Opt. Express*, vol. 21, pp. 3201–12, 2013.
[7] J. W. Pan, Y. C. Su, and Y. S. Chen, “Secondary optical element design for intracorporeal LED illumination system,” *Opt. Lett.*, vol. 39, pp. 224–227, 2014.
[8] J. J. Vos, “On the cause of disability glare and its dependence on glare angle, age and ocular pigmentation,” *Clin. Express Optometry*, vol. 86, no. 6, pp. 363–370, 2010.
[9] T. Kasahara, D. Aizawa, T. Moriyama, M. Toda, and M. Iwamoto, “Discomfort glare caused by white LED light sources,” *J.Light Vis. Env.*, vol. 30, no. 2, pp. 95–103, 2006.
[10] A. Travis, N. Emerton, and S. Bathiche, “Collimated light from a waveguide for a display backlight,” *Opt. Express*, vol. 17, no. 22, pp. 19714–19719, 2009.
[11] J. A. Wheatley *et al.*, “Efficient LED light distribution cavities using low loss, angle-selective interference transflectors,” *Opt. Express*, vol. 17, no. 13, pp. 10612–10622, 2009.
[12] C. C. Sun *et al.*, “Calculating model of light transmission efficiency of diffusers attached to a lighting cavity,” *Opt. Express*, vol. 18, no. 6, pp. 6137–6148, 2010.
[13] O. Dross, J. C. Miñano, P. Benitez, A. Cvetkovic, and J. Chavez, “Non-imaging optics combine LEDs into one bright source,” *Int. Soc. Opt. Eng.*, 2006.
[14] P. Gimenez-Benitez *et al.*, “Simultaneous multiple surface optical design method in three dimensions,” *Opt. Eng.*, vol. 43, no. 7, pp. 1489–1502, 2004.
[15] J. L. Alvarez *et al.*, “TIR-R concentrator: A new compact high-gain SMS design,” in *Proc. Spie Int. Soc. Opt. Eng.*, 2001, Art. no. 4446.
[16] P. Gu *et al.*, “Freeform LED lens for uniform illumination,” *Opt. Express*, vol. 16, no. 17, 2008, Art. no. 12958.
[17] Y. Ding, P. F. Gu, and Z. R. Zheng, “The freeform reflector for uniform rectangular illumination,” *Japanese J. Appl. Phys. Part 1, Regular Papers, Brief Commun. Rev. Papers*, vol. 46, no. 12, pp. 7771–7773, 2007.
[18] Z. M. Zhu *et al.*, “Uniform illumination design by configuration of LED array and diffuse reflection surface for color vision application,” *J. Display Technol.*, vol. 7, no. 2, pp. 84–89, 2011.
[19] Z. M. Zhu *et al.*, “Design of diffuse reflection freeform surface for uniform illumination,” *J. Display Technol.*, vol. 10, no. 1, pp. 7–12, 2014.
[20] Z. M. Zhu, H. Liu, and S. M. Chen, “The design of diffuse reflective freeform surface for indirect illumination with high efficiency and uniformity,” *IEEE Photon. J.*, vol. 7, no. 3, 2015, Art. no. 1600510.
[21] Z. Zhu, “Uniform illumination study by light-emitting diode ring array and diffuse reflection surface,” *Acta Optica Sinica*, vol. 31, no. 1, 2011, Art. no. 0115001.
[22] Z. M. Zhu, X. Sun, and B. Peng, “The design of diffuse reflective off-axis surface for noncircular LED arrays,” *IEEE Photon. J.*, vol. 9, no. 1, 2017, Art. no. 1600210.
[23] W. E. Vargas, “Optimization of the diffuse reflectance of pigmented coatings taking into account multiple scattering,” *J. Appl. Phys.*, vol. 88, no. 7, pp. 4079–4084, 2000.
[24] Z. Zhu *et al.*, “Design method of double freeform surface lens with diffuse reflection,” *Lighting Res. Technol.*, 2019.